Environ Geochem Health (2022) 44:1259–1275
https://doi.org/10.1007/s10653-021-01138-z

ORIGINAL PAPER

Preparation of chitosan/sodium alginate/nano cellulose composite for the efficient removal of cadmium (II) cations from wastewater and soil systems

Sara Mola ali abasiyan · Azar Nasiri Sour · Amir Mokhtari · Farahnaz Dashbolaghi · Mohammad Sabzi

Received: 7 February 2021 / Accepted: 15 October 2021 / Published online: 29 October 2021

Abstract In this study, chitosan/sodium alginate/nano cellulose (CSA-N) nanocomposite hydrogels were prepared using a completely green route and used as sorbents to adsorb Cd^{2+} ions from water and soil systems of an environmental aspect. The sorbents were characterized by FTIR, SEM, and XRD. The influences of initial Cd^{2+} concentration, the presence of nano cellulose, type of the polluted environment, and ionic strength on adsorption and desorption isotherms were investigated. The maximum adsorption capacity of cadmium onto CSA was significantly increased from 2264.9 to 4380.97 µmol/g when the system was changed from soil to water, respectively. While, the maximum adsorption capacity of cadmium onto CSA-N was almost the same in the soil and wastewater systems, i.e., 3419.5 and 3230.3 µmol/g, respectively. The results indicated that Langmuir and Freundlich models provided the best fit for the experimental adsorption data for CSA and CSA-N, respectively. By comparing the amounts of Δq, the difference between adsorption and desorption amounts, the CSA was not economically feasible sorbent at high initial concentrations of Cd^{2+} in the wastewater system, while, CSA-N was demonstrated to be a more efficient adsorbent than CSA for cadmium removal from both the soil and wastewater systems.

Keywords Polysaccharides · Nanocomposite · Cadmium (II) removal · Wastewater · Soil · Adsorption isotherm

Abbreviations

CSA-N	Chitosan-sodium alginate loaded with nano cellulose
CSA	Chitosan-sodium alginate hydrogels without cellulose
EC	Electrical conductivity
OM	Organic matter
FTIR	Fourier-transform infrared spectroscopy
XRD	X-ray powder diffraction
SEM	Scanning electron microscopy

Introduction

The probability of contaminating water and soil resources with heavy metals is increased by raising the industrial activity. The acceptable limit of Cd^{2+} in wastewater is 0.0889 µmol L^{-1} (Musyoka et al.,

S. Mola ali abasiyan (✉) · A. Nasiri Sour · F. Dashbolaghi
Department of Soil Sciences, Soil Chemistry Laboratory, Faculty of Agriculture, University of Maragheh, P. O. Box 55181-83111, Maragheh, Iran
e-mail: abasiyan@maragheh.ac.ir

A. Mokhtari · M. Sabzi
Department of Chemical Engineering, Faculty of Engineering, University of Maragheh, Maragheh 55181-83111, Iran

2011). Nickel–cadmium batteries, fertilizers, mining, stabilizers, and alloys are the main sources of cadmium ions in the environment (Dabrowski et al. 2004). Different processes such as chemical precipitation (Alvarez et al., 2007), membrane separation (Kheriji et al., 2015), coagulation (Escobar et al., 2006), ion exchange (Dabrowski et al. 2004), and adsorption (Ahmad et al., 2019; Kaveeshwar et al., 2018; Shou et al., 2016; Xu & Wang, 2017) have been used for removal of heavy metals such as cadmium from water and wastewater systems. On the other hand, risks of causing secondary pollutants are associated with the majority of these methods. Removal of metal ions by adsorption using biomaterials lessens these risks (Peretz et al., 2015; Wang & Chen, 2006, 2009). Besides, this method has many advantages, such as low initial cost, process simplicity, and local availability (Papageorgiou et al., 2009). Natural materials such as chitosan, zeolites, clay, or certain waste products from industrial operations such as fly ash, coal, and oxides are arranged as low-cost adsorbents.

Chitosan is a biomaterial that has been collected from crustaceans and fungal biomass (Igberase et al., 2014) and used for the removal of cadmium ions (Li et al., 2017; Ramya et al., 2012). However, chitosan is soluble in acidic pHs, which hinders its usage in many applications. In order to overcome this issue, various cross-linked chitosan systems, such as glutaraldehyde cross-linked chitosan, epichlorohydrin cross-linked chitosan (Kamari et al., 2011), magnetic chitosan/κ-carrageenan nanocomposites (Mola ali abasiyan et al., 2019), and also chitosan-based biosorbents (Wang & Chen, 2014; Wang & Zhuang, 2017; Zhuang et al., 2021) have been developed for heavy metal removal. Alginate is another useful biomaterial to remove metals from water, which the main responsible functional groups for the removal of the metal are carboxyl and hydroxyl groups. It should be noted that metal ions such as cadmium prefer to be adsorbed to carboxyl groups rather than to hydroxyl groups of alginates (Qin et al., 2007; Wang et al., 2016). Cellulose is a long linear polysaccharide polymer consisting of glucose units. It is an important component of the plant cell wall. Cellulose is a biodegradable and eco-friendly natural polymer extracted from plants and trees (Yue et al., 2019). Pure cellulose has less ability as an adsorbent compared to its modified form (Jorge & Chagas, 1988).

Babel and Kurniawan reported that carboxymethyl cellulose and sodium alginate as hydrogels based on bio-resources were efficient to omit heavy metals from contaminated water in comparison to other common adsorbents such as activated carbon (Babel & Kurniawan, 2003). The removal of Pb^{2+}, Cd^{2+}, Ni^{2+}, and Cu^{2+} from aqueous solutions using sodium alginate-g-poly (AMPS-co-AA-co-AM) was explored (Mohammad et al., 2017). It was found that the adsorption mechanism is better described by Langmuir isotherm model and the maximum adsorption capacity is 4062.09 μmol g^{-1} for cadmium ion.

In the present work, chitosan-sodium alginate loaded with nano cellulose (CSA-N) and chitosan-sodium alginate hydrogels without nano cellulose (CSA) were produced and used as the sorbents. This work aims to evaluate the potential of these biopolymers to be used as the sorbents and soil amendments in wastewater and soil systems, respectively. In wastewater system, the effects of different ionic strengths were also investigated. It is worth to note that, based on our literature review, this is the first report on the application of the chitosan/alginate/nano cellulose nanocomposite as an efficient sorbent for cadmium removal, especially from soil system.

Experimental

Materials

Chitosan (CS, with of viscosity 20–300 cps, for 1 wt% in 1% aqueous solution of acetic acid, degree of deacetylation ≥ 75%) and sodium alginate (SA, medium molecular weight, viscosity ≥ 2,000 cps, for 2 wt% in H_2O) were obtained from Sigma-Aldrich Co., USA. To prepare a stock solution, 2.74 g Cd $(NO_3)_2{\cdot}4H_2O$ in 1 L deionized was dissolved, and to obtain more dilute solutions, the stock solution was diluted.

Preparation of sorbents

Ionic crosslinking can occur during the fabrication of bionanocomposites due to opposite charge of sodium alginate (SA) and chitosan (CS) biopolymers. The chitosan/sodium alginate/cellulose nano fibers (CS/SA/NFs) hydrogels (CSA-N) were prepared by adding

the SA and CS powders into distilled water (1 wt%) and 2 vol% acetic acid aqueous solution (2 wt%) under mixing with a magnetic stirrer for 2 h, respectively. Subsequently, the CS solution was drope-wisely added to the SA solution within 5 h, leading to form a polyelectrolyte complex due to protonated amino groups of CS and negatively charged carboxylate groups of SA. Afterward, NFs suspension (20 wt%) was drop-wisely added in to the CS/SA solution and ultrasonicated (Development of Ultrasonic Technology Co., Iran) for 5 min, followed by stirring over night at ambient temperature. At last, the resultant solution was casted and dried. The resultant samples were immersed in $CaCl_2$ solution (100 mL, 10 wt%) for post-crosslinking of SA chains, as schematically shown in Fig. 1. Ultimately, the samples were rinsed with distilled water and dried at ambient condition. CS/SA hydrogels (CSA) were prepared with the same method, except no cellulose NFs were added.

Tested soil

The soil sample used in this research was the same as our recent work (Mola ali abasiyan et al., 2019). As mentioned in the previous work, some chemical properties of the soil, such as pH, electrical conductivity (EC), and organic matter content (OM), were determined following standard laboratory methods (Soil Survey Staff, 2004) and found to be 7.6, 0.64 ds/m, and 0.88%, respectively.

Isotherm studies of Cd^{2+} in the systems by the CSA and CSA-N sorbents

Adsorption of cadmium on CSA and CSA-N sorbents were investigated using batch experiments. The CSA or CSA-N (0.55 g L^{-1}) was tightly capped and equilibrated 10 h at 20 ± 1 °C in 0.00266 mol L^{-1} Ca $(NO_3)_2.4H_2O$ as a controlling ionic strength at pH 7.6 (the pH of all samples was adjusted to 7.6 in both water and soil systems due to the natural pH of soil samples being 7.6) with different cadmium concentrations from 0 to 1.9768 mmol L^{-1}. The pH was adjusted during the experiment. Blank samples were used to eliminate the other parameters in the systems. To separate the adsorbent from the suspension after equilibration, centrifuging for 15 min at 10,000 rpm was applied. Atomic absorption spectrophotometer (Shimadzu, AA- 6300) was used to measure the concentration of cadmium in the supernatant. The difference in the concentration of added cadmium and the final equilibrium concentration was considered as the cadmium sorption. In order to calculate the equilibrium adsorption capacities (q_e, μmol/g), the

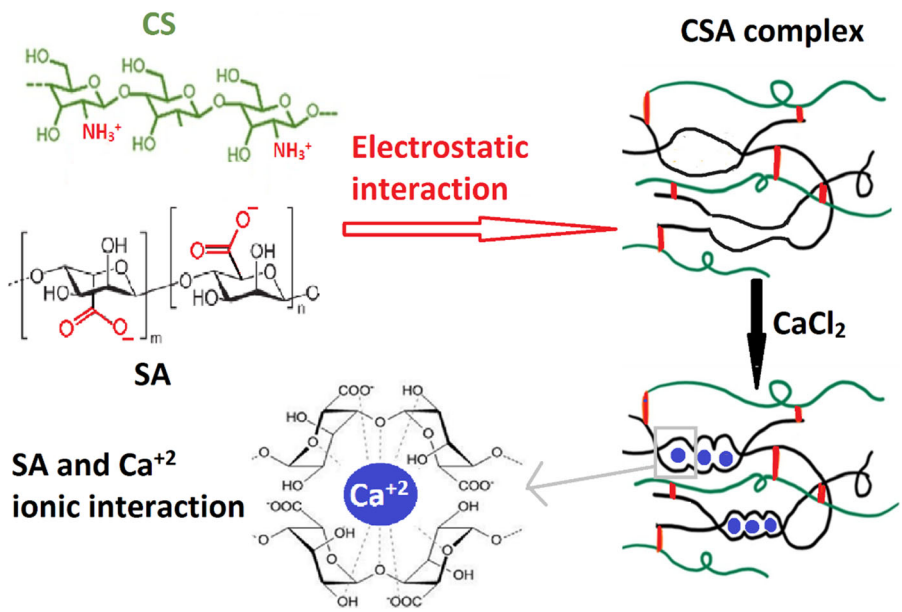

Fig. 1 Schematic representation of structure of CS, SA, and post-crosslinking of CSA complex by $CaCl_2$

differences between initial concentration (C_o, µmol/L) and final concentration (C_e, µmol/L) of Cd^{2+} at equilibrium time was used (Eq. 1).

$$q_e = \frac{C_o - C_e}{m} \times V \quad (1)$$

where V (L) and m (g) are the volume of Cd^{2+} solution used for adsorption process and the weight of the used sorbent, respectively.

To investigate the desorption studies, the CSA and CSA-N loaded with cadmium ions were washed with distilled water and treated with HCl (Igberse and Osifo 2015). Atomic absorption spectrophotometer (Shimadzu, AA- 6300) was used to measure the amount of Cd^{2+} desorption. The percentage of desorption was calculated by Eq. 2 from the previous work (Mola ali abasiyan et al., 2019). These adsorption–desorption experiments in the soil system were conducted with the same method used for wastewater system, except adding definite soil (5.55 g L^{-1}) (Garcia-Miragaya & Page, 1978).

To investigate ionic strength effect, 0.0026 and 0.0080 mol L^{-1} $Ca(NO_3)_2{\cdot}4H_2O$ were used in wastewater system as a background electrolyte at pH 7.6 with different cadmium concentrations.

Characterization

Dried and ground bioadsorbents were mixed with dry KBr powder, and their FTIR (Shimadzu 8400S, Japan) spectra were obtained from their KBR pellets within 4000–500 cm^{-1}.

The structure and crystalline state of bioadsorbents were evaluated by using a JEOL X-ray diffractometer apparatus (JDX-8030, Japan) at a wavelength of 1.54 Å (Cu-Kα) and a voltage of 40 kV and a current of 44 mA. Cross-sectional micrographs of the gold-sputtered bioadsorbents were obtained by using a field emission-scanning electron microscope (MIRA3 FE-SEM, Tescan, Czech).

Results and discussion

Characterization of adsorbents

In the FTIR spectrum of chitosan, a wide band at 3090–3540 cm^{-1} is assigned to the stretching vibrations of O–H and N–H bonds. The bands appeared at 2854 and 2915 cm^{-1} are attributed to stretching vibration of C–H bonds. The shoulder around 1640 cm^{-1} is originated from scissoring vibration of absorbed water and carbonyl stretching (amide I) vibration of this polysaccharide. The band located at 1581 cm^{-1} is correlated to the bending vibration of N–H (residues of N-acetylated, amide II band). The bands at 1433 and 1386, and 1151 cm^{-1} are corresponding to C–H bending, O–H bending, and anti-symmetric stretching of C–O–C bridge vibration, respectively (Pourjavadi et al., 2020; Shaheen et al., 2019). The characteristic bands of SA at 3351, 1605, 1410, and 1084 cm^{-1} are attributed to stretching of –OH, asymmetric stretching of COO^-, symmetric stretching of COO^-, and stretching of C–O, respectively (Zhao et al., 2021).

FTIR spectrum of cellulose NFs shows a broad band in the range of 3050–3670 cm^{-1} originated from stretching vibration of hydroxyl groups (Fig. 2a). The band in the region of 1310–1380 cm^{-1} arose from in-plane bending of COH and CCH. In addition, the spectrum exhibited bands in the range of 970–1180 cm^{-1} correlated to the C-O, C–O–C, and C–C stretching vibrations, and the band at 1159 cm^{-1} can be assigned to C–O–C stretching of glycosidic bonds (Melo et al., 2018).

In the spectrum of CS/SA polyelectrolyte complex (CSA) and its corresponding nanocomposite (CSA-N), the band at 1581 cm^{-1} originated from scissoring vibration of NH_2 in chitosan is disappeared and a band at 1550 cm^{-1} originated from NH_3^+ groups is appeared due to involving in electrostatic interactions with alginate (Pourjavadi et al., 2020; Shaheen et al., 2019). In addition, symmetrical COO^- band of SA at 1410 cm^{-1} became wider and asymmetrical COO^- band of SA at 1605 cm^{-1} shifted to a lower wavenumber and merged with the band of NH_3^+ groups at 1550 cm^{-1} due to complexation in CSA.

The XRD patterns of CSA and its corresponding nanocomposite containing cellulose NFs were shown in Fig. 2b. XRD patterns of CSA showed a strong peak at 27.03°, relating to the crystalline nature of SA. Two typical peaks at 10.6° and 20.6° proved the crystallinity of CS (Lin et al., 2015). Moreover, distinguished sharp diffraction peak at 37.69° is attributed to the crystalline phase of SA (Shao et al., 2018). By incorporation of CNF as a filler into matrix, the CSA-N spectrum illustrated additional peaks at 16.3° and

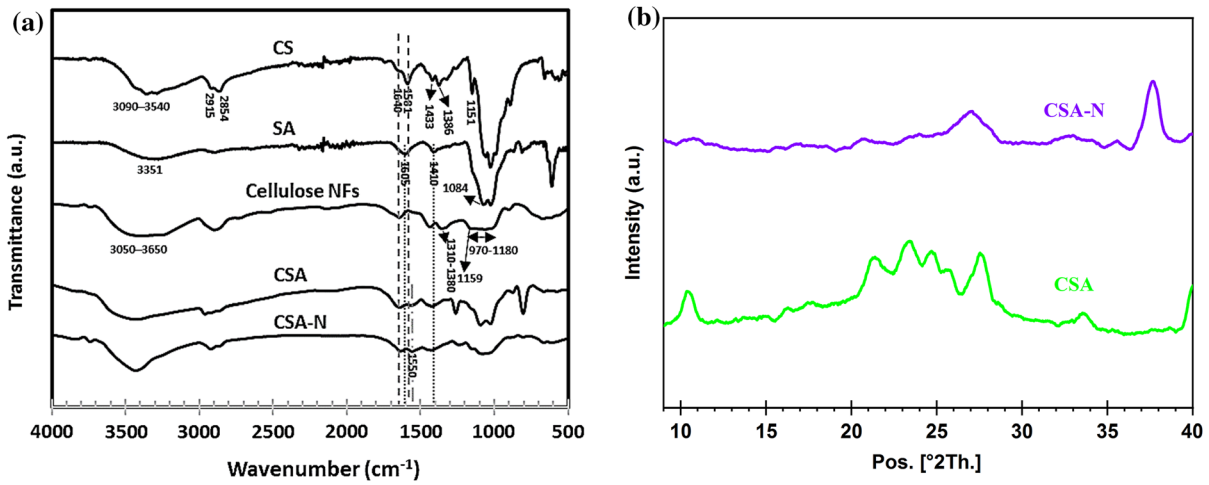

Fig. 2 **a** FTIR spectra of chitosan (CS), sodium alginate (SA), nano cellulose NFs, chitosan-sodium alginate (CSA), and chitosan-sodium alginate with cellulose NFs (CSA-N); **b** XRD patterns of CSA and CSA-N

20–25.61°, demonstrating the high degree of crystallinity of CNF (Huq et al., 2012).

SEM analysis was used for examining the morphologies of fractured surfaces of CS/SA with and without CNF (Fig. 3). Showing the dispersion of CNF into the matrix and appearing noticeable changes at the presence of CNF with different magnification.

According to Figs. 3a, b, the fractured surface of CS/SA is approximately rough and has negligible porosity. But its roughness and porosity increased with incorporation of cellulose NFs, which would be a beneficial and favorable feature for a bioadsorbent during heavy metal ions removal (Hu et al., 2018). Some bright speckles in Fig. 3c, d can be correlated to the presence of cellulose NFs in the matrix. Absence of any phase separation and agglomeration in the cross-section of the nanocomposite can be indicative of well-dispersion of cellulose NFs in the matrix due to intermolecular hydrogen bonding between the filler and matrix (Celebi & Kurt, 2015; Ghourbanpour et al., 2019).

SEM micrographs of the Cd^{2+} adsorbed by CSA and CSA-N and their corresponding EDX mappings of Ca, Cd, and N elements were displayed in Fig. 4. It can be seen that Ca and N elements, as indicatives of the $CaCl_2$ crosslinker and chitosan, respectively, were uniformly distributed within the matrix. Besides that, it is evident from Fig. 4c, f that the Cd^{2+} ions were uniformly adsorbed and diffused throughout the both sorbents.

Isotherm studies of Cd^{2+} in the vicinity of CSA sorbent

In this work, four isotherm models were employed, namely: Freundlich (it is a physical adsorption model), Langmuir (this model is a theoretical monolayer chemical adsorption), Dubinin–Radushkevich (D–R) (this model is a semi-empirical model on the basis of Polanyi's theory), and Temkin (it is an empirical model) models to fit experimental data of Cd^{2+} adsorption and desorption (Wang & Guo, 2020). The equations are given in detail in our previous paper (Mola ali abasiyan et al., 2019).

The values of constants together with correlation coefficient (r^2) and RMSE for forth models for CSA bio adsorbents in wastewater system with different ionic strengths are listed in Table 1. In the ionic strength of 8 mM, the correlation coefficient for the adsorption of Cd^{2+} by CSA sorbent in the wastewater system is 0.997, 0.999, 0.550, and 0.720 and the RMSE is 31.06, 34.74, 555.40, and 295.20 for Freundlich, Langmuir, D-R, and Temkin equations, respectively. The correlation coefficient for the desorption of Cd^{2+} in the same system is 0.97, 0.65, 0.69, and 0.87 and the RMSE is 8.24, 27.87, 37.99, and 16.69 for Freundlich, Langmuir, D-R, and Temkin equations, respectively. In the ionic strength 24 mM, the correlation coefficient for the adsorption of Cd^{2+} by CSA bio adsorbent in the wastewater system is 0.995, 0.998, 0.26, and 0.68 and the RMSE is 24.87, 20.66, 378.11, and 201.97 for Freundlich, Langmuir,

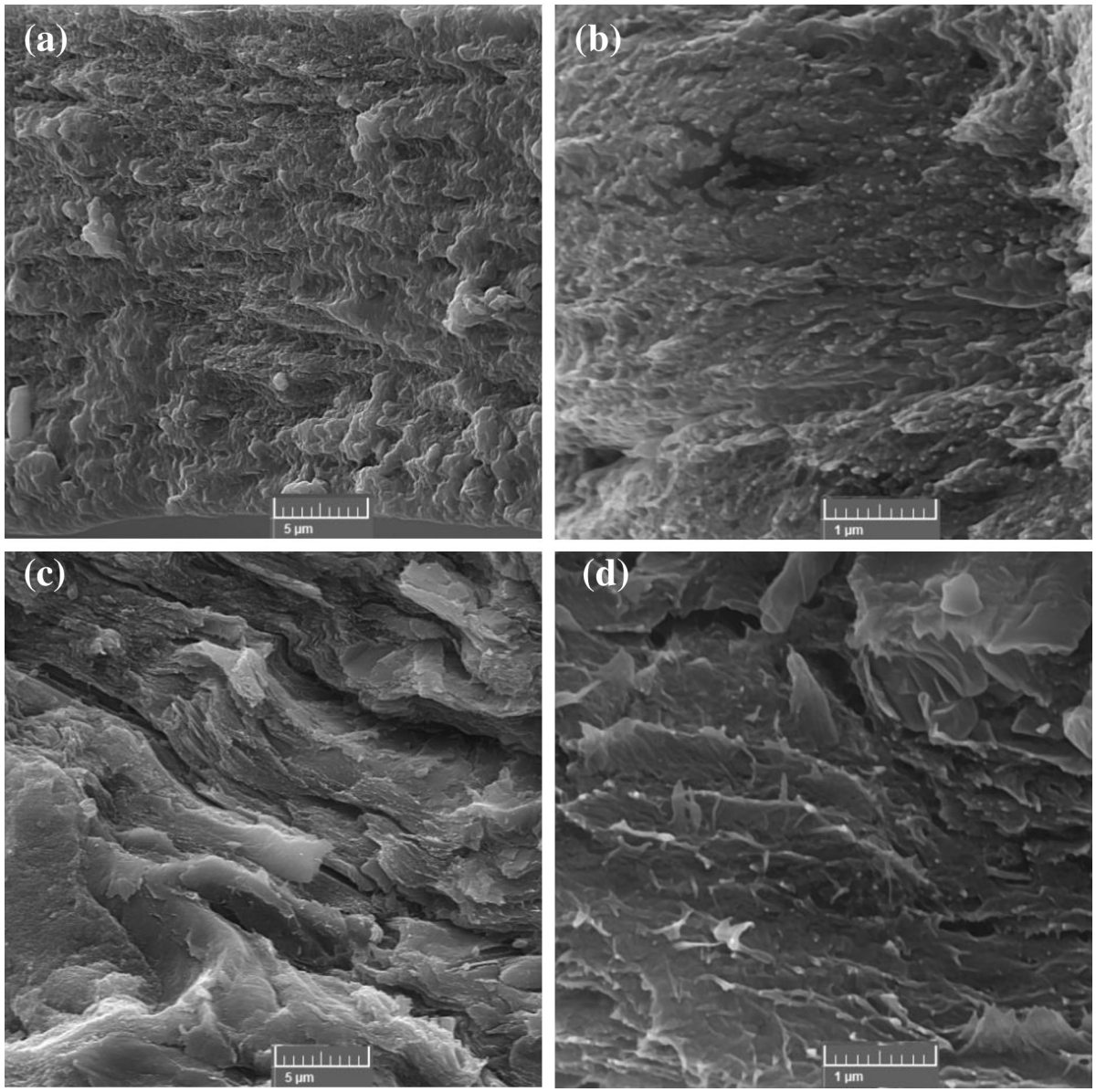

Fig. 3 SEM micrographs of (**a**) and (**b**) CSA composite, **c** and **d** CSA-N nanocomposite at different magnification

D-R, and Temkin equations, respectively. The correlation coefficient for the desorption of Cd^{2+} in the same system is 0.995, 0.985, 0.290, and 0.790, and the RMSE is 7.75, 13.81, 114.50, and 51.22 for Freundlich, Langmuir, D-R, and Temkin equations, respectively. Based on analyzing the obtained values of r^2 and RMSE using four models for CSA sorbent, it can be found that Langmuir model provided the best fit for the experimental adsorption and desorption data in the studied concentration range of the Cd^{2+}in both applied ionic strengths (Fig. 5a, b). When the level of ionic strength changed from the lowest to the highest value, the maximum adsorption capacity (b) of Cd^{2+} onto CSA decreased from 4380.97 to 2530.25 µmol/g, respectively. A similar trend was observed in our previous study on the adsorption of Cd^{2+} by polyvinyl alcohol/ laponite RD hydrogel nanocomposite (PVA-mLap2) (Mola ali abasiyan & Mahdavinia, 2018), and the maximum adsorption capacity of Cd^{2+} onto PVA-

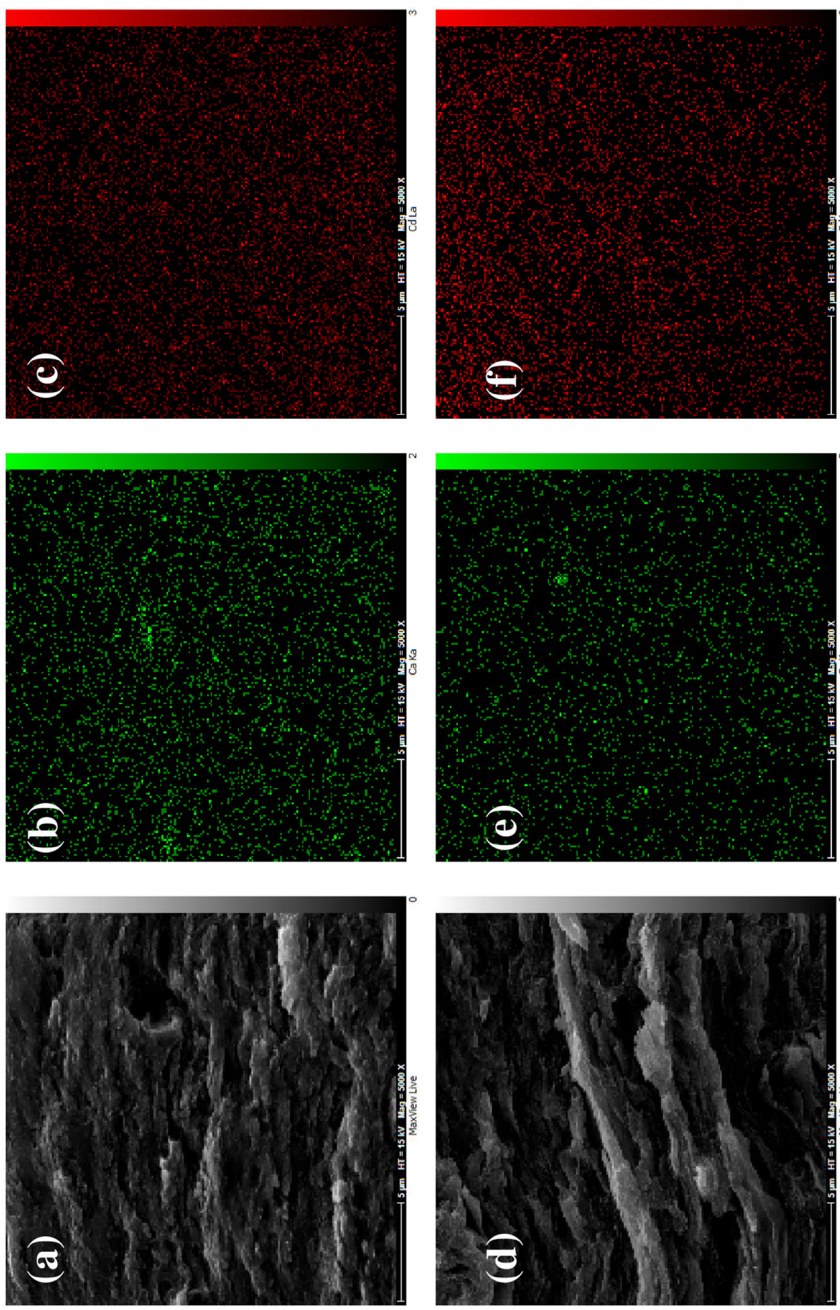

Fig. 4 **a** SEM micrograph of Cd^{2+} adsorbed CS-SA and its corresponding EDX mapping of **b** Ca, **c** Cd and **d** N elements. **e** SEM micrograph of Cd^{2+} adsorbed CS-SA-N nanocomposite and its corresponding EDX mapping of **f** Ca, **g** Cd and **h** N elements

Table 1 Parameters of the Freundlich, Langmuir, Dubinin-Radushkerich, and Temkin models for Chitosan-Sodium Alginate (CSA) in wastewater system with different ionic strength

Model	Parameter	Wastewater system(I = 8 mM)		Wastewater system (I = 24 mM)	
		Adsorption	Desorption	Adsorption	Desorption
Freundlich	n	0.79	0.39	0.76	0.56
	K_F	7.50	9.83	4.69	6.17
	r^2	0.997	0.970	0.995	0.995
	RMSE	31.06	8.24	24.87	7.75
Langmuir	B (μmol/g)	4380.97	9256.07	2530.25	478.95
	K	0.0006	1.88×10^{-5}	0.0006	0.0017
	r^2	0.9989	0.65	0.998	0.985
	RMSE	34.74	27.87	20.66	13.81
Dubinin-Radushkerich	Q_m (μmol/L)	250.26	65.04	124.75	69.52
	B (mol^2/KJ^2)	5.7×10^{-6}	3.6×10^{-6}	1.25×10^{-6}	1.02×10^{-6}
	E (KJ/mol)	295.05	370.9	631.22	701.17
	r^2	0.55	0.69	0.26	0.29
	RMSE	555.40	37.99	378.11	114.50
Temkin	B (J/mol)	241.98	21.28	144.33	46.11
	b_T	10.06	114.45	16.88	52.83
	AT (L/g)	0.1309	0.4095	0.1223	0.2032
	r^2	0.72	0.87	0.68	0.79
	RMSE	295.20	16.69	201.97	51.22

mLap2 was obtained to be 119 μmol/g in 0.006 M and 80 μmol/g in 0.025 M ionic strength, respectively.

Since soil has a complex nature and the addition of any substance for control of ionic strength can have different side effects, therefore in this study, the natural ionic strength of the soil itself, i.e., the ionic strength of 0.008 M, has been considered. The value of constants along with correlation coefficients (r^2) and RMSE values obtained from four models for CSA bio adsorbents in the soil system were listed in Table 2. The correlation coefficients for the adsorption of Cd^{2+} by CSA sorbent in the soil system are 0.989, 0.980, 0.790, and 0.930 and the RMSE values are 69.69, 85.36, 286.86, and 95.50 for Freundlich, Langmuir, D-R, and Temkin equations, respectively. The correlation coefficients for the desorption of Cd^{2+} in the same system are 0.97, 0.97, 0.79, and 0.93 and the RMSE are 58.65, 56.80, 286.86, and 95.50 for Freundlich, Langmuir, D-R, and Temkin equations, respectively. Based on analyzing the values of r^2 and RMSE obtained using four models for CSA bio adsorbent, it can be found that Langmuir and Freundlich models provided the best fit for the experimental adsorption and desorption data, respectively, in the studied concentration range of Cd^{2+}in soil system (Fig. 6a, b). Even though the amounts of cadmium sorption onto CSA were more in the soil system as compared with the wastewater system in the same ionic strength (I = 0.008 M), the maximum adsorption capacity (b) of cadmium onto CSA appeared to decrease from the wastewater system to the soil system from 4380.97 to 2264.90 μmol/g, respectively (Fig. 6a, b). The amounts of cadmium sorption were more in the soil system as compared with the wastewater system. This phenomenon can be associated with the presence of organic materials as additional adsorbents in the soil system. Heavy metals can be held by soil organic matter due to the presence of functional groups such as carboxyl, carbonyl, and phenolic. (Tipping, 2002). As shown in Fig. 7a, the slope of the curve in the wastewater system is greater than that of the soil system. In the soil system, the adsorption amounts remain almost constant after the equilibrium concentration of 400 μmol/L. While, in

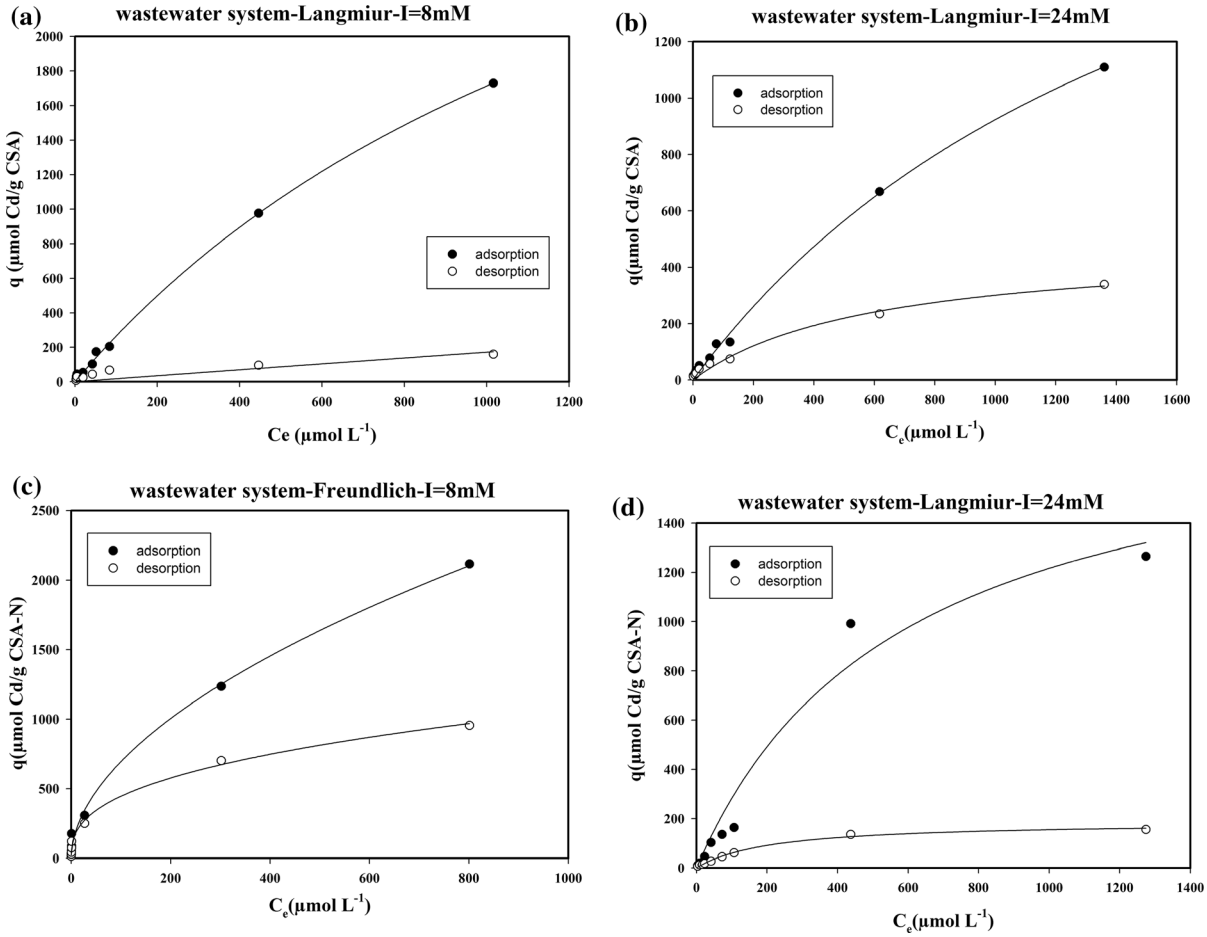

Fig. 5 **a** and **b** the best fit for Isotherms of adsorption and desorption of Cd (II) by CSA in 8 and 24 mM ionic strength, respectively; **c** and **d** are the best fit for Isotherms of adsorption and desorption of Cd (II) by CSA-N in 8 and 24 mM ionic strength, respectively, in the wastewater system (T = 20 °C, adsorption dose = 0.55 g L^{-1}, pH = 7.6, cadmium concentrations of 0–1976.8 µmol L^{-1})

the wastewater system, under the same condition, the amount of adsorption is still increasing with higher equilibrium concentrations. This can account for the observed higher maximum absorption in the wastewater system as compared to that of the soil system.

Isotherm studies of Cd^{2+} in the vicinity of CSA-N sorbent

The value of constants along with correlation coefficient (r^2) and RMSE of four models for CSA-N bio adsorbents in the wastewater system with different ionic strengths was listed in Table 3. In 8 mM ionic strength, r^2 for the adsorption of Cd^{2+} by CSA-N bio adsorbent in the wastewater system was 0.995, 0.985, 0.750, and 0.835 and the RMSE was 48.47, 86.97, 618.16, and 291.08 for Freundlich, Langmuir, D–R, and Temkin equations, respectively. The correlation coefficients for the desorption of Cd^{2+} in the same system were 0.994, 0.969, 0.810, and 0.920 and the RMSE were 25.90, 58.08, 253.46, and 95.16 for Freundlich, Langmuir, D-R, and Temkin equations, respectively. In 24 mM ionic strength, r^2 for the adsorption of Cd^{2+} by CSA-N bio adsorbent in the wastewater system was 0.93, 0.97, 0.34, and 0.78 and the RMSE was 121.80, 79.69, 469.80, and 207.07 for Freundlich, Langmuir, D–R, and Temkin equations, respectively. The desorption studies in the wastewater system were indicated with r^2 values of 0.94, 0.99,

Table 2 Parameters of the Freundlich, Langmuir, Dubinin-Radushkerich, and Temkin models for Chitosan-Sodium Alginate with and without nano cellulose in the soil system

Model	Parameter	CSA-without nano cellulose		CSA-N	
		Adsorption	Desorption	Adsorption	Desorption
Freundlich	n	0.42	0.33	0.49	0.39
	K_F	121.53	117.16	85.67	83.22
	r^2	0.989	0.970	0.999	0.995
	RMSE	69.69	58.65	24.12	17.50
Langmuir	b (μmol/g)	2264.90	1021.07	3230.30	741.17
	K	0.0070	0.0260	0.0029	0.0270
	r^2	0.980	0.970	0.977	0.966
	RMSE	85.36	56.80	113.03	47.29
Dubinin-Radushkerich	q_m (μmol/L)	466.10	344.80	295.60	169.70
	B (mol^2/KJ^2)	1.75×10^{-7}	1.63×10^{-7}	2.4×10^{-10}	2.06×10^{-10}
	E (KJ/mol)	1688.9	1749.2	45,624.5	49,234.2
	r^2	0.74	0.79	0.26	0.28
	RMSE	597.40	286.86	782.70	264.09
Temkin	B (J/mol)	211.74	116.58	23.12	9.14
	b_T	11.5	20.9	105.3	266.5
	A_T (L/g)	2.13	2.92	5.61×10^{11}	7.9×10^{12}
	r^2	0.85	0.93	0.18	0.24
	RMSE	252.8	95.5	671.3	225.4

0.39, and 0.89 and with the RMSE values of 13.16, 4.40, 50.98, and 17.07 for Freundlich, Langmuir, D-R, and Temkin equations, respectively. Based on analyzing the values of r^2 and RMSE obtained from the applied models in CSA-N bio adsorbent, it is found that Freundlich and Langmuir models will be the best fits for the experimental adsorption and desorption data in 8 mM (Fig. 5c) and 24 mM ionic strengths (Fig. 5d), respectively. When the level of ionic strength changed from the lowest to the highest value, the maximum adsorption capacity (b) of Cd^{2+} onto CSA-N appeared to decrease from 3419.50 to 1924.73 μmol/g, respectively. The same results were found for cadmium adsorption on CSA.

The value of constants along with r^2 and RMSE of four models for CSA-N bio adsorbents in the soil system were also listed in Table 2. In the soil system, r^2 for cadmium adsorption by CSA-N bio adsorbent were 0.999, 0.977, 0.260, and 0.180 and the RMSE were 24.12, 113.03, 782.70, and 671.30 for Freundlich, Langmuir, D–R, and Temkin equations, respectively. The correlation coefficients for the desorption of Cd^{2+} in the same system were 0.995, 0.966, 0.280, and 0.240 and the RMSE were 17.50, 47.29, 264.09, and 225.40 for Freundlich, Langmuir, D-R, and Temkin equations, respectively. In the vicinity of CSA-N bio adsorbent in the soil system, the results indicated that Freundlich model was the best fit by analyzing the values of r^2 and RMSE for the applied models (Fig. 6c). The results show that the amount of cadmium sorption onto CSA-N in the wastewater system was likely the same as in the soil system. As indicated in Tables 2 and 3, the maximum adsorption capacity (b) was almost the same in the soil and wastewater systems, i.e., 3419.5 and 3230.3 μmol/g, respectively (Fig. 7b). However, the amount of cadmium adsorption onto CSA-N seems to be higher in the soil system in comparison to the wastewater system due to the presence of organic materials in the soil. One of the possible reasons for this phenomenon could be due to partial decomposition of nano cellulose/sodium alginate/chitosan in the soil.

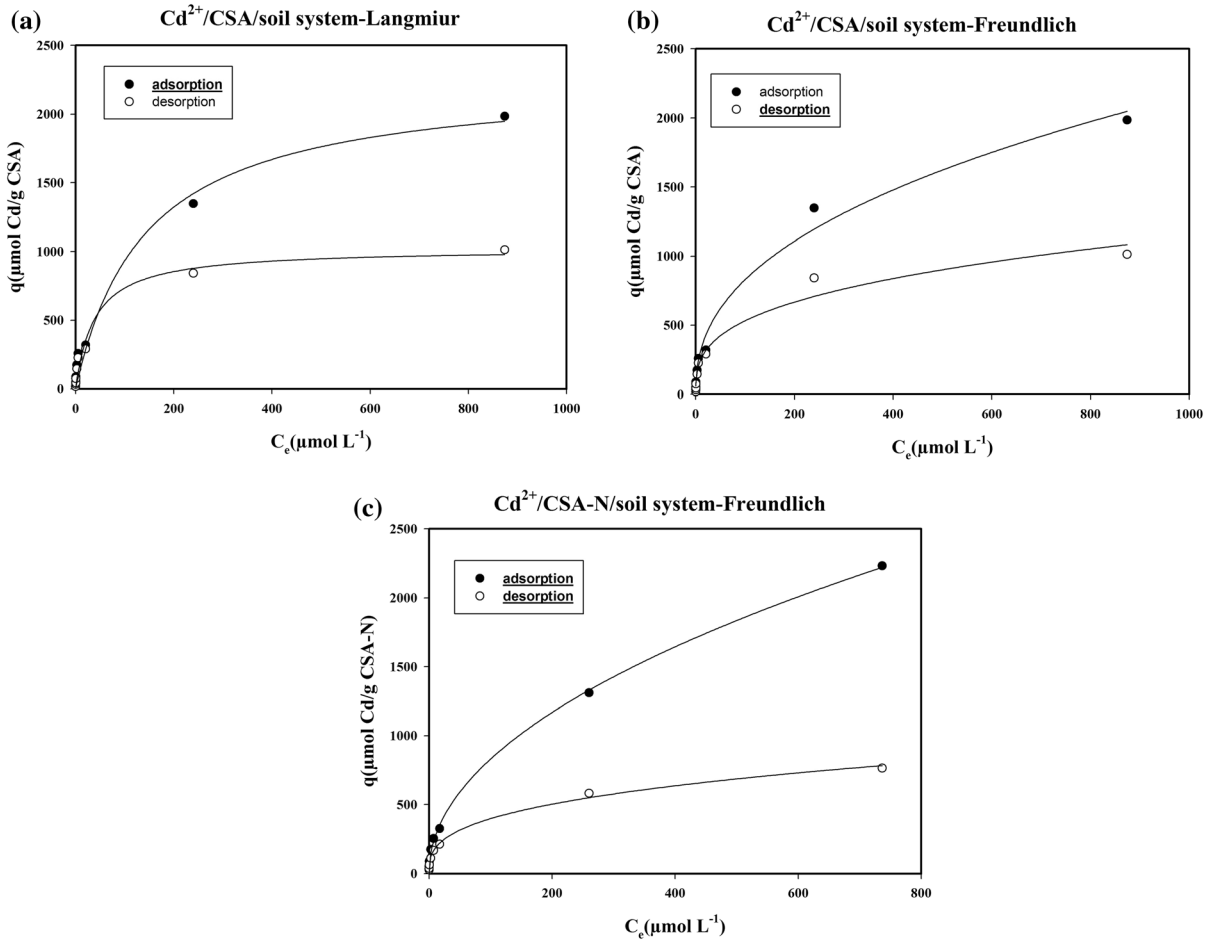

Fig. 6 **a** and **b** the best fit for Isotherms of adsorption and desorption of Cd (II) by CSA in soil system, respectively; **c** the best fit for Isotherms of adsorption and desorption of Cd (II) by CSA-N in soil system (in defined conditions as the same Fig. 5)

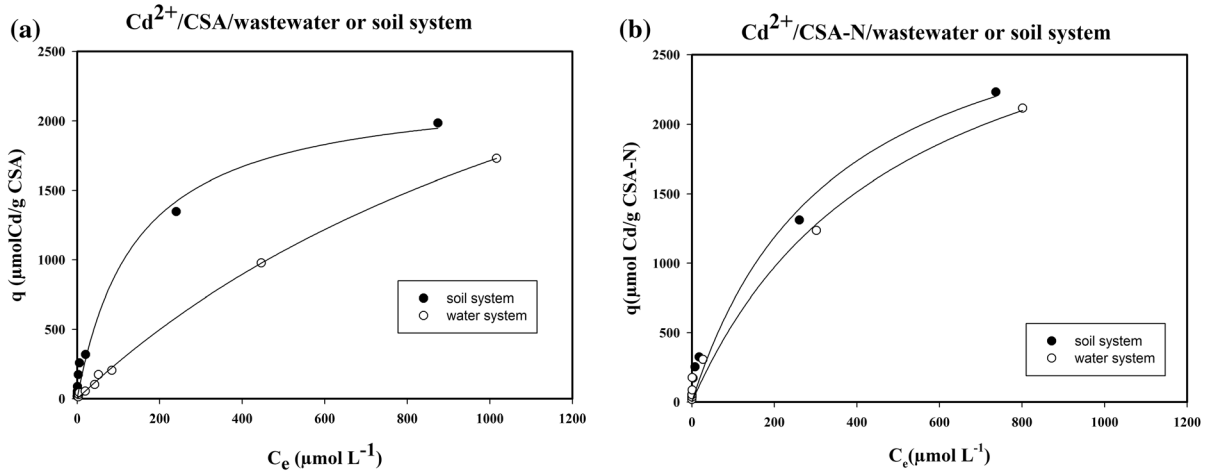

Fig. 7 **a** Comparison of the cadmium adsorptions in the CSA-water and CSA-soil systems and **b** in CSA-N-water and CSA-N-soil systems

Table 3 Parameters of the Freundlich, Langmuir, Dubinin-Radushkerich, and Temkin models for Chitosan-Sodium Alginate-Nano cellulose in wastewater system with different ionic strengths

Model	Parameter	Wastewater system(I = 8 mM)		Wastewater system (I = 24 mM)	
		Adsorption	Desorption	Adsorption	Desorption
Freundlich	n	0.53	0.37	0.64	0.45
	K_F	59.8	79.7	14.2	6.7
	r^2	0.995	0.994	0.930	0.940
	RMSE	48.47	25.90	121.80	13.16
Langmuir	b (μmol/g)	3419.50	1031.10	1924.73	187.30
	K	0.0020	0.0096	0.0017	0.0048
	r^2	0.9850	0.9690	0.9700	0.9900
	RMSE	86.97	58.08	79.69	4.40
Dubinin-Radushkerich	q_m (μmol/L)	538.83	348.70	147.28	43.19
	B (mol^2/KJ^2)	1.84×10^{-7}	1.72×10^{-7}	8.67×10^{-6}	5.99×10^{-6}
	E (KJ/mol)	1648.63	1706.60	240.15	288.80
	r^2	0.75	0.81	0.34	0.39
	RMSE	618.16	253.46	469.80	50.98
Temkin	B (J/mol)	209.66	102.51	226.49	28.45
	b_T	11.62	23.76	10.76	85.63
	A_T (L/g)	2.7200	3.5500	0.0760	0.1271
	r^2	0.835	0.920	0.780	0.890
	RMSE	291.08	95.16	207.07	17.07

To determine the heterogeneity of adsorption sites on the adsorbent surface, n constant in the Freundlich equation is measured (Sposito, 1980). Surface site heterogeneity increases whenever n reaches 0, this represents a wide distribution of a variety of adsorption sites. Conversely, as n approaches unity, surface site homogeneity increases, showing that there is a narrow distribution of adsorption site types. The results indicate that the amount of n is higher in the wastewater system than in the soil system in the vicinity of CSA and CSA-N. It is important to understand that, by increasing the complication of adsorbents in the same condition in both adsorbents, i.e., CSA and CSA-N, the heterogeneity of adsorption sites is increased. It should be noted that the difference between the amount of n in CSA and CSA-N is considerable in the wastewater system. In the wastewater system, the n constant for CSA and CSA-N is 0.79 and 0.53, respectively. It means the surface of CSA adsorbent has more homogeneity than the surface of CSA-N adsorbent.

Dubinin-Radushkevich model was used to determine the mechanistic of reaction by using potential theory. The assumption of this model is that the surface of the adsorbent is heterogeneous. By using D-R model, if the adsorption free energy's value (E) is less than 8 kJ/mol, it will mean physical adsorption (Kundu & Gupta, 2006), if the value of E becomes between 8 and 16 kJ/mol, it will express ion-exchange process (Helfferich, 1962), and if the value of E is more than 16 kJ/mol, it will indicate chemisorption process(Chen et al., 2010). In this work, the values of E are 295.05 and 1688.90 kJ/mol for the cadmium adsorption in the vicinity of CSA in the water and soil system, respectively; 1648.6 and 45,624.5 kJ/mol for the cadmium adsorption in the vicinity of CSA-N in water and soil system, respectively, which indicates the adsorption of cadmium onto CSA and CSA-N surfaces are following chemical adsorption type in the both studied systems. The results indicate that adsorption free energy's value (E) has a significant increase in the soil system in comparison to the wastewater system in both adsorbents, especially in CSA-N. It is

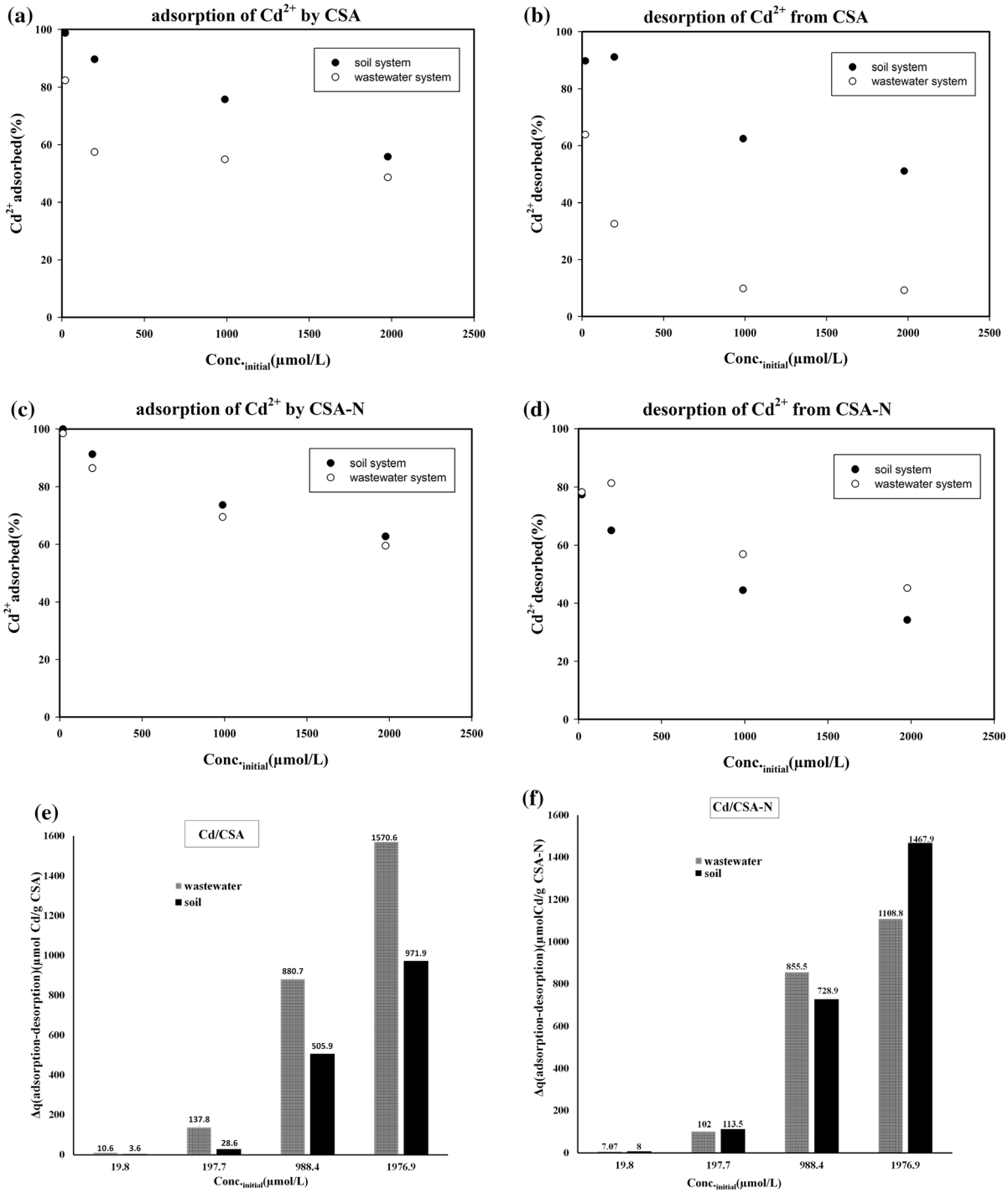

Fig. 8 **a**,**b** Adsorption–desorption of Cd^{2+} on CSA in the systems; **c**,**d** Adsorption–desorption of Cd^{2+} on CSA-N in water and soil systems; **e**,**f** Δq as a function of the Cd^{2+} initial concentration in the presence of CSA and CSA-N bio adsorbent (in defined conditions as the same Fig. 5)

related to the existence of strong binding of cadmium onto CSA-N in the vicinity of organic materials in the soil system.

To evaluate the efficiency of two adsorbents by comparing two systems

The effects of initial Cd^{2+} concentrations on Cd^{2+} adsorption and desorption by CSA and CSA-N in the two systems were indicated in Fig. 8a–d, respectively. In both studied systems and in both adsorbents, the percentages of cadmium adsorption were reduced by rising initial Cd^{2+} concentrations. In the CSA sorbent, by rising initial cadmium concentrations from 20 to 2000 μmol L^{-1} in the soil system, cadmium adsorption decreased from 98.7 to 55.8%. The corresponding decrease from 82.3 to 48.6% in the same range of initial Cd^{2+} concentrations was observed in the wastewater system. In CSA-N sorbent, cadmium adsorption decreased from 100 to 62.7% by rising initial Cd^{2+} concentrations in the soil system. The corresponding decrease from 98.5 to 48.6% in the same range of initial Cd^{2+} concentrations was obtained in the wastewater system. The results showed in both sorbents, cadmium adsorption follows the same trend. Furthermore, by escalating initial cadmium concentrations, cadmium desorption percentage decreased in both adsorbents and both the studied systems. In the CSA sorbent, Cd^{2+} desorption decreased from 89.7 to 51.0% with an increase in initial Cd^{2+} concentration from 20 to 2000 μmol L^{-1} in the soil system. The corresponding decrease from 63.9 to 9.2% in the same range of initial Cd^{2+} concentrations was observed in the wastewater system. In the CSA-N sorbent, Cd^{2+} desorption decreased from 77.4 to 34.2% with an increase in initial Cd^{2+} concentration from 20 to 2000 μmol L^{-1} in the soil system. The corresponding decrease from 78.2 to 45.1% in the same range of initial Cd^{2+} concentrations was achieved in the wastewater system. The results indicated the adsorption percentage decreased with increasing initial Cd^{2+} concentrations in both sorbents. This phenomenon can be related to the possibility of greater availability of adsorption sites for cadmium ions at low values of initial cadmium concentration, and hence all cadmium ions can be bound to the sites. The results indicated that both CSA and CSA-N are good sorbents toward cadmium ions in both systems, and there is no noticeable difference in the adsorption amounts of the studied systems. The amount of the Cd^{2+} adsorption onto CSA-N is slightly higher than CSA in both the systems. When the desorption percentages of the two adsorbents are compared. This is the conclusion that can be drawn that the desorption of cadmium onto CSA-N in the wastewater system is relatively higher than that of the soil system, whereas a contrary result was obtained in the case of CSA (Fig. 8). This indicates that CSA-N is more appropriate adsorbent of cadmium in the wastewater system due to its efficient regeneration as compared with CSA.

To investigate the efficiency of the developed materials as efficient sorbents in water and soil systems, the difference between adsorption and desorption amount, Δq, was calculated and shown in Fig. 8e, f. In a water system, it is important to use the adsorbent several times, so the lower the amounts of Δq, the better the adsorbent's ability to reuse. But in a soil system, the adsorbent's ability to immobilize definite heavy metal ions is important. Therefore, the lower the amounts of Δq, the better the adsorbent's ability to immobilize the metal ions. It was clear from Fig. 8e, f that the Δq of both adsorbents was increased in both systems when the cadmium initial concentration was raised. In the wastewater system, the Δq value of CSA is higher than that of CSA-N adsorbent. Therefore, this indicates that CSA-N with a smaller Δq value is a more efficient adsorbent for cadmium in water. Furthermore, the Δq of CSA-N in the soil system is larger than that of the CSA adsorbent. As it was mentioned before, the larger Δq value in a soil system, the adsorbent will be more efficient to remove cadmium by immobilization method. As a result, CSA-N is a more efficient adsorbent than CSA adsorbent for cadmium removal in both the soil and wastewater systems.

Conclusions

In the present work, ionically chitosan/sodium alginate hydrogels containing nano cellulose (CSA-N) and chitosan-sodium alginate hydrogels without nano cellulose (CSA) were successfully prepared using a green and facile method without the need for any toxic crosslinkers and organic solvents. It was indicated that the CSA and CSA-N can be considered as efficient sorbents of Cd^{2+} in both the systems. The maximum

adsorption capacity (B parameter in Tables) of cadmium onto CSA was significantly increased from 2264.9 to 4380.97 μmol/g when the system was changed from soil to water, respectively. While, B parameter of cadmium onto CSA-N was almost same in the soil and wastewater systems, i.e., 3419.5 and 3230.3 μmol/g, respectively. Based on analyzing the obtained values of r^2 and RMSE using Freundlich, Langmuir, Dubinin-Radushkevich, and Temkin models. It was found that Langmuir and Freundlich models provided the best fit for the experimental adsorption data for CSA and CSA-N, respectively. By comparing the amounts of Δq, the difference between adsorption and desorption amounts, the CSA was not economically feasible sorbent at high initial concentrations of Cd^{2+} in the wastewater system, while CSA-N was demonstrated to be a more efficient adsorbent than CSA for cadmium removal from both the soil and wastewater systems.

Author contributions Dr S and Mr M prepared the adsorbents. Mrs NS and D performed laboratory analysis. Dr MA abasiyan analyzed and interpreted the data; wrote the manuscript. All authors read and approved the final manuscript.

Funding Not applicable.

Availability of data and material Data and material are indicated in the manuscript. However, if the reviewers need more detail, we can provide it.

Code availability To plot figures, use SigmaPlot 10 and Excel 2016.

Declarations

Conflict of interest The authors declare that they have no known competing financial interests or personal relationships that could have appeared to influence the work reported in this paper.

References

Ahmad, Z. U., Lian, Q., Zappi, M. E., Buchireddy, P. R., & Gang, D. D. (2019). Adsorptive removal of resorcinol on a novel ordered mesoporous carbon (OMC) employing COK-19 silica scaffold: Kinetics and equilibrium study. *Journal of Environmental Sciences, 75*, 307–317.

Alvarez, M. T., Crespo, C., & Mattiasson, B. (2007). Precipitation of Zn (II), Cu (II) and Pb (II) at bench-scale using biogenic hydrogen sulfide from the utilization of volatile fatty acids. *Chemosphere, 66*(9), 1677–1683.

Babel, S., & Kurniawan, T. A. (2003). Low-cost adsorbents for heavy metals uptake from contaminated water: A review. *Journal of Hazardous Materials, 97*(1–3), 219–243.

Celebi, H., & Kurt, A. (2015). Effects of processing on the properties of chitosan/cellulose nanocrystal films. *Carbohydrate Polymers, 133*, 284–293.

Chen, H., Dai, G., Zhao, J., Zhong, A., Wu, J., & Yan, H. (2010). Removal of copper (II) ions by a biosorbent-Cinnamomum camphora leaves powder. *Journal of Hazardous Materials, 177*(1–3), 228–236.

Dabrowski, A., Hubicki, Z., Podkościelny, P., & Robens, E. (2004). Selective removal of the heavy metal ions from waters and industrial wastewaters by ion-exchange method. *Chemosphere*, *56*(2), 91-106.

Escobar, C., Soto-Salazar, C., & Toral, M. I. (2006). Optimization of the electrocoagulation process for the removal of copper, lead and cadmium in natural waters and simulated wastewater. *Journal of Environmental Management, 81*(4), 384–391.

Garcia-Miragaya, J., & Page, A. L. (1978). Sorption of trace quantities of cadmium by soils with different chemical and mineralogical composition. *Water Air Soil Pollution, 9*(3), 289–299.

Ghourbanpour, J., Sabzi, M., & Shafagh, N. (2019). Effective dye adsorption behavior of poly (vinyl alcohol)/chitin nanofiber/Fe (III) complex. *International Journal of Biological Macromolecules, 137*, 296–306.

Helfferich, F. (1962). Theories of ion-exchange column performance: A critical study. *Angewandte Chemie International Edition in English, 1*(8), 440–453.

Hu, Z. H., Omer, A. M., Ouyang, X. K., & Yu, D. (2018). Fabrication of carboxylated cellulose nanocrystal/sodium alginate hydrogel beads for adsorption of Pb (II) from aqueous solution. *International Journal of Biological Macromolecules, 108*, 149–157.

Huq, T., Salmieri, S., Khan, A., Khan, R. A., Le Tien, C., Riedl, B., Fraschini, C., Bouchard, J., Uribe-Calderon, J., Kamal, M. R., & Lacroix, M. (2012). Nanocrystalline cellulose (NCC) reinforced alginate based biodegradable nanocomposite film. *Carbohydrate polymers, 90*(4), 1757–1763.

Igberase, E., Osifo, P., & Ofomaja, A. (2014). The adsorption of copper (II) ions by polyaniline graft chitosan beads from aqueous solution: Equilibrium, kinetic and desorption studies. *Journal of Environmental Chemical Engineering, 2*(1), 362–369.

Igberase, E., & Osifo, P. (2015). Equilibrium, kinetic, thermodynamic and desorption studies of cadmium and lead by polyaniline grafted cross-linked chitosan beads from aqueous solution. *Journal of Ind Eng Chem, 26*, 340–347.

Jorge, R. A., & Chagas, A. P. (1988). Ion-exchange equilibria between solid aluminium pectinates and Ca, Mn II, Cu II and Fe III ions in aqueous solution. *Journal of the Chemical Society, Faraday Transactions 1: Physical Chemistry in Condensed Phases*, *84*(4), 1065–1073.

Kamari, A., Pulford, I. D., & Hargreaves, J. S. J. (2011). Binding of heavy metal contaminants onto chitosans–an evaluation for remediation of metal contaminated soil and water. *Journal of Environmental Management, 92*(10), 2675–2682.

Kaveeshwar, A. R., Kumar, P. S., Revellame, E. D., Gang, D. D., Zappi, M. E., & Subramaniam, R. (2018). Adsorption

properties and mechanism of barium (II) and strontium (II) removal from fracking wastewater using pecan shell based activated carbon. *Journal of Cleaner Production, 193*, 1–13.

Kheriji, J., Tabassi, D., & Hamrouni, B. (2015). Removal of Cd (II) ions from aqueous solution and industrial effluent using reverse osmosis and nanofiltration membranes. *Water Science and Technology, 72*(7), 1206–1216.

Kundu, S., & Gupta, A. K. (2006). Arsenic adsorption onto iron oxide-coated cement (IOCC): Regression analysis of equilibrium data with several isotherm models and their optimization. *Chemical Engineering Journal, 122*(1–2), 93–106.

Li, B., Zhou, F., Huang, K., Wang, Y., Mei, S., Zhou, Y., & Jing, T. (2017). Environmentally friendly chitosan/PEI-grafted magnetic gelatin for the highly effective removal of heavy metals from drinking water. *Scientific Reports, 7*, 43082.

Lin, S., Chen, L., Huang, L., Cao, S., Luo, X., & Liu, K. (2015). Novel antimicrobial chitosan–cellulose composite films bioconjugated with silver nanoparticles. *Industrial Crops and Products, 70*, 395–403.

Melo, B. C., Paulino, F. A., Cardoso, V. A., Pereira, A. G., Fajardo, A. R., & Rodrigues, F. H. (2018). Cellulose nanowhiskers improve the methylene blue adsorption capacity of chitosan-g-poly (acrylic acid) hydrogel. *Carbohydrate Polymers, 181*, 358–367.

Mohammad, N., Atassi, Y., & Tally, M. (2017). Synthesis and swelling behavior of metal-chelating superabsorbent hydrogels based on sodium alginate-g-poly (AMPS-co-AA-co-AM) obtained under microwave irradiation. *Polymer Bulletin, 74*(11), 4453–4481.

Mola ali abasiyan, S. M. A., Dashbolaghi, F., & Mahdavinia, G. R. (2019). Chitosan cross-linked with κ-carrageenan to remove cadmium from water and soil systems. *Environmental Science and Pollution Research*, *26*(25), 26254-26264.

Mola Ali Abasiyan, S., & Mahdavinia, G. R. (2018). Polyvinyl alcohol-based nanocomposite hydrogels containing magnetic laponite RD to remove cadmium. *Environmental Science and Pollution Research International, 25*(15), 14977–14988.

Musyoka, S. M., Ngila, J. C., Moodley, B., Petrik, L., & Kindness, A. (2011). Synthesis, characterization, and adsorption kinetic studies of ethylenediamine modified cellulose for removal of Cd and Pb. *Analytical Letters, 44*(11), 1925–1936.

Papageorgiou, S. K., Katsaros, F. K., Kouvelos, E. P., & Kanellopoulos, N. K. (2009). Prediction of binary adsorption isotherms of Cu2+, Cd2+ and Pb2+ on calcium alginate beads from single adsorption data. *Journal of Hazardous Materials, 162*(2–3), 1347–1354.

Peretz, S., Anghel, D. F., Vasilescu, E., Florea-Spiroiu, M., Stoian, C., & Zgherea, G. (2015). Synthesis, characterization and adsorption properties of alginate porous beads. *Polymer Bulletin, 72*(12), 3169–3182.

Pourjavadi, A., Doroudian, M., Bagherifard, M., & Bahmanpour, M. (2020). Magnetic and light-responsive nanogels based on chitosan functionalized with Au nanoparticles and poly (N-isopropylacrylamide) as a remotely triggered drug carrier. *New Journal of Chemistry, 44*(40), 17302–17312.

Qin, Y., Cai, L., Feng, D., Shi, B., Liu, J., Zhang, W., & Shen, Y. (2007). Combined use of chitosan and alginate in the treatment of wastewater. *Journal of Applied Polymer Science, 104*(6), 3581–3587.

Ramya, R., Sudha, P. N., & Mahalakshmi, J. (2012). Preparation and characterization of chitosan binary blend. *International Journal of Scientific and Research Publications, 2*(10), 1–9.

Shaheen, T. I., Montaser, A. S., & Li, S. (2019). Effect of cellulose nanocrystals on scaffolds comprising chitosan, alginate and hydroxyapatite for bone tissue engineering. *International Journal of Biological Macromolecules, 121*, 814–821.

Shao, Y., Chunhua, W., Tiantian, W., Yuan, C., Chen, S., Ding, T., Ye, X., & Yaqin, H. (2018). Green synthesis of sodium alginate-silver nanoparticles and their antibacterial activity. *International Journal of Biological Macromolecules, 111*, 1281–1292.

Shou, W., Chao, B., Ahmad, Z. U., & Gang, D. D. (2016). Ordered mesoporous carbon preparation by the in situ radical polymerization of acrylamide and its application for resorcinol removal. *Journal of Applied Polymer Science*. https://doi.org/10.1002/app.43426

Soil Survey Staff (2004) Soil survey laboratory methods manual-Soil Survey Investigations Report No. 42. USDA-NRCS, Lincolon

Sposito, G. (1980). Derivation of the Freundlich equation for ion exchange reactions in soils. *Soil Science Society of America Journal, 44*(3), 652–654.

Tipping, E. (2002). *Cation binding by humic substances* (Vol. 12). Cambridge University Press.

Wang, J., & Chen, C. (2006). Biosorption of heavy metals by Saccharomyces cerevisiae: A review. *Biotechnology Advances, 24*(5), 427–451.

Wang, J., & Chen, C. (2009). Biosorbents for heavy metals removal and their future. *Biotechnology Advances, 27*(2), 195–226.

Wang, J., & Chen, C. (2014). Chitosan-based biosorbents: Modification and application for biosorption of heavy metals and radionuclides. *Bioresource Technology, 160*, 129–141.

Wang, F., Lu, X., & Li, X. Y. (2016). Selective removals of heavy metals (Pb^{2+}, Cu^{2+}, and Cd^{2+}) from wastewater by gelation with alginate for effective metal recovery. *Journal of Hazardous Materials, 308*, 75–83.

Wang, J., & Zhuang, S. (2017). Removal of various pollutants from water and wastewater by modified chitosan adsorbents. *Critical Reviews in Environmental Science and Technology, 47*(23), 2331–2386.

Wang, J., & Guo, X. (2020). Adsorption isotherm models: Classification, physical meaning, application and solving method. *Chemosphere, 258*, 127279.

Xu, L., & Wang, J. (2017). The application of graphene-based materials for the removal of heavy metals and radionuclides from water and wastewater. *Critical Reviews in Environmental Science and Technology, 47*(12), 1042–1105.

Yue, X., Huang, J., Jiang, F., Lin, H., & Chen, Y. (2019). Synthesis and characterization of cellulose-based adsorbent for removal of anionic and cationic dyes. *Journal of Engineered Fibers and Fabrics, 14*, 1558925019828194.

Zhao, X., Wang, X., & Lou, T. (2021). Preparation of fibrous chitosan/sodium alginate composite foams for the adsorption of cationic and anionic dyes. *Journal of Hazardous Materials, 403*, 124054.

Zhuang, S., Zhu, K., & Wang, J. (2021). Fibrous chitosan/cellulose composite as an efficient adsorbent for Co (II) removal. *Journal of Cleaner Production, 285*, 124911.